

# Histopathological and Immunohistochemical Study of Antiosteoporotic Efficacy of the Earthworm *Allolobophora caliginosa* Extract in Orchiectomized Rats

Estudio Histopatológico e Inmunohistoquímico de la Eficacia Antiosteoporótica del Extracto de Lombriz de Tierra *Allolobophora caliginosa* en Ratas Orquiectomizadas

Ayat Magdy; Sohair Ramadan Fahmy; Ayman Saber Mohamed; Dalia Y. Saad;  
Reham S. Desokyand & Ahmed Abdel Aziz Baiomy

---

MAGDY, A.; FAHMY, S. R.; MOHAMED, A. S.; SAAD, D. Y.; DESOKYAND, R. S. & BAIOMY, A. A. A. Histopathological and immunohistochemical study of antiosteoporotic efficacy of the earthworm *Allolobophora caliginosa* extract in orchiectomized rats. *Int. J. Morphol.*, 40(1):277-286, 2022.

**SUMMARY:** Osteoporosis is a bone condition marked by a loss of bone mass and a disruption of bone microarchitecture. Men lose bone density as they age, resulting in brittle bones. The loss of free testosterone is one of the key factors. The objective of present study was to evaluate *Allolobophora caliginosa* extract (AcE) for its anti-osteoporotic and antiapoptotic activity in orchiectomized rat model at two different dose levels. Twenty eight male rats were divided into two groups. The first group represented sham operated rats while the second group underwent bilateral orchidectomy (OCX). After one week of recovery from orchidectomy surgery, the second group was randomly subdivided into 3 subgroups. The first OCX subgroup was administered orally distilled water daily for 10 weeks. The other two OCX subgroups were administered AcE (100 or 200 mg/kg body weight/day) orally for 10 weeks. Orchiectomy induces remarkable loss of the cortical as well as trabecular bone loss; which, could be counterbalanced by *Allolobophora caliginosa* extract (AcE) that prevented cortical as well as trabecular bone loss. *Allolobophora caliginosa* extract (AcE) at Dose 200 mg/kg/day was found to be effective at a highly significant level in osteoporotic bone, as determined by histological images and immunohistochemical study, where Dose (100 mg/kg/day) was found to be moderately significant. In the present study, it is suggested that AcE may inhibit steroid-induced osteoblasts apoptosis, potentially via upregulation of Bcl-2 and downregulation of caspase-3. *Allolobophora caliginosa* extract demonstrates anti-apoptotic and anti-oxidant properties. Therefore, AcE may be used for the prevention of steroid-induced bone damage.

**KEY WORDS:** Osteoporosis; *Allolobophora caliginosa* extract; Orchiectomized rat; Histopathology; Apoptosis.

---

## INTRODUCTION

Bone is a vital dynamic tissue that undergoes frequent remodeling with the specific end goal of replacing old and micro-damaged bone with new, mechanically stronger bone. This procedure is performed using harmoniously balanced groups of bone resorbing osteoclasts and bone-forming osteoblasts (Bai *et al.*, 2019).

Osteoporosis (OP) is characterized as a reduction in bone mass and a degradation of bone architecture that leads to a bone-thinning with direct effects on increased cortical porosity, bone fragility, and fracture risk (Qaseem *et al.*, 2017).

With age, there is gradual bone loss in men associated with a decrease in hormone levels. Androgens may play an important role in the regulation of bone formation in men

(Khosla, 2010; Qaseem *et al.*). Men are also affected by estrogen changes due to aging, as testosterone is the precursor to estrogen. Estrogen is believed to play a greater role in bone resorption (Saki *et al.*, 2019). Orchiectomized rats have been shown to have an increase in bone resorption markers, suggesting a role for testosterone deficiency (Sakr *et al.*, 2020).

In fact, the presence of active caspase-3-positive cells is thought to be a sign of apoptosis activation (Baiomy & Mansour, 2016; Badr *et al.*, 2020).

Bcl-2 is a member of the antiapoptotic protein family that can inhibit or slow down cell death caused by a series of stimuli (Kale *et al.*, 2018).

Testosterone and bisphosphonates are of the most common antiresorptive agents used to treat osteoporosis (Chen & Sambrook, 2011; Fui et al., 2018). Treatment with testosterone not only increased BMD but also increased prostate gland size and levels of prostate specific antigen (Duque & Troen, 2008).

Bisphosphonate use has also been linked to esophageal cancer, gastrointestinal problems, and jaw osteonecrosis (Kuehn, 2009; Li & Zhong, 2020).

The earthworm's body cavity contains coelomic fluid, which has several anti-inflammatory activities (Bin Dajem et al., 2020). Earthworm (*Pheretima asperillum*) extract stimulates osteoblast activity and inhibits osteoclast differentiation (Fu et al., 2014).

Therefore, the ongoing study was carried out to investigate the antiosteoporotic and antiapoptotic effect of the earthworm *Allolobophora caliginosa* extract (AcE) in orchidectomized rats (OCX).

## MATERIAL AND METHOD

**Collection of Earthworms.** Earthworms of species *Allolobophora caliginosa* were collected from a commercial vermiculture at Giza Governorate and maintained in plastic tubs containing decomposed organic matter until used for study.

**Preparation of earthworm extract.** Five hundred adult clitellated worms (900 mg/worm) were kept in 0.65 % NaCl at room temperature for 1~2 h until their digestive systems became clean with a few times of solution changes. Animals were kept out of the solution and minced with scissors. Three grams of earthworm tissue was homogenized in 40 ml of chloroform-methanol solution and left overnight at 4 °C. The following day, 16 ml of distilled water was added to the homogenate. Then the mixture was centrifuged at 2460×g for 10 min. Three clearly visible layers were obtained. The upper, water/methanol layer was pipetted out and evaporated on a rotavapor until no methanol was left. An opalescent fluid, pH 7, was obtained, freeze-dried and kept at 4 °C until use (Hrzenjak et al., 1992).

**Animals.** Adult male Wistar albino rats (*Rattus norvegicus*) weighing 150 - 170 g were obtained from the animal house of the National Research Center (NRC), Egypt. Rats were housed in polypropylene cages in air-conditioned room at a temperature of 23 ± 2 °C and under natural day and night cycle. They were fed standard chow pellets and drinking

water ad libitum. The rats were kept for a week before the commencement of the experiment for acclimatization.

**Orchiectomy and Sham Operation Procedure.** Anesthesia was induced with 50 mg/kg sodium pentobarbital that was injected intra-peritoneally for generalized anesthesia. Bilateral orchiectomy was performed via a scrotal approach. The anesthetized rat was placed supine on the operating table and its position was fixed using sticking tape. The scrotal hair was bilaterally shaved. A small, 1.0-cm median incision was made through the skin at the tip of the scrotum. The cremaster muscles were opened with a small, 7-mm incision. At the entrance to the scrotal cavity, the testicular fat pad was located and pulled through the incision using blunt forceps. The cauda epididymis was pulled out along with the testis, followed by the caput epididymis, the vas deferens and the testicular blood vessels. The testis and epididymis were removed. This procedure was repeated for on the other testis and epididymis. The cremaster muscle and scrotal skin were sutured layer by layer. The same preparation was performed on animals in the sham operation group, allowing the authors to visually identify the testis, epididymis, vas deferens and testicular blood vessels. After visual identification, the cremaster muscle and skin were sutured without ligation or resection.

**Experimental design.** All animal procedures were evaluated and approved by Ethical committee Office of Faculty of Sciences, Cairo University, Egypt (Registration number: CU-I-F-53-18).

Twenty eight male rats were divided into two groups. The first group (7 rats/group) represented sham operated rats while the second group (21 rats/group) underwent bilateral orchidectomy (OCX). After one week of recovery from orchidectomy surgery, the second group was randomly subdivided into 3 subgroups (7 rats/ each subgroup). The first OCX subgroup was administered orally distilled water (vehicle) daily for 10 weeks. The other two OCX subgroups were administered orally *Allolobophora caliginosa* extract (AcE) (100 or 200 mg/kg body weight/day) for 10 weeks.

**Histopathology of femur bone:** At the end of the experimental period, the animals were killed and the femoral bones of the selected rats from each group were used to analyze the bone histopathology by hematoxylin-eosin (HE) staining. Briefly, the left femur bone samples were fixed in 10 % formalin for 24 h followed by 4-week decalcification at 4C by 10 % ethylene diamine tetraacetic acid (EDTA) solution. After that, bone samples were washed, dehydrated in ascending concentrations of ethanol, cleared with xylene, infiltrated and embedded in paraffin wax. Thin sections of 5 mm thick using a rotary microtome. Sections were stained with Hematoxylin

& Eosin stains (H&E) for light microscope examination of micro-architecture of femur bone (Kumar, 2014) .

**Immunohistochemistry.** Sections were deparaffinized and rehydrated through xylene and serial dilutions of EtOH to distilled H<sub>2</sub>O. They were then incubated in Antigen Retrieval Citra (Biogenex; San Ramon, CA) at 95°C for 15 min. Sections were washed in PBS, pH 7.4, with 0.02 % Triton X-100 (PBS) twice for 3 min each. All incubations were performed in a humidity chamber at room temperature and followed by two, 3-min washes in PBS, and then incubated with anti-Bcl-2 (diluted 1:200, Santa Cruz Biotechnology, Santa Cruz, CA, USA), anti-caspase-3 (diluted 1:200, Abcam, Cambridge, MA, USA) antibodies overnight at 4°C as primary antibodies. After rinsing with phosphate buffered saline, they were incubated with the appropriate biotinylated secondary antibodies according to the Vecta stain Elite ABC Kit (Vector Laboratories, Burlingame, CA, USA) for 30 min at room temperature. The immune reactions were visualized by using diaminobenzidine (DAB, Sigma Chemical Co, St. Louis, Missouri, USA) under light microscopy and then counterstained with Mayer's hematoxylin (Sigma-Aldrich, St. Louis, MO, USA) followed by routine dehydration in alcohol, clearing in xylene, and mounting using the Aquatex fluid (Merk KGaA, Darmstadt, Germany) under a cover slip. Semi-quantification analysis of apoptotic expression represented by the percentage of positively immune stained cells (brown cytoplasm for Bcl-2 and brown nucleus for caspase-3) by counting at least 100 cells per slide, subdivided into 10 random fields.  $A\% = (\text{number of positive cells} / \text{total number of calculated cells})$  (Hassanein *et al.*, 2019).

**Scanning electron microscopy (SEM) of femur bone.** For SEM evaluations, the proximal parts of the femora were trimmed in a coronal plane. They were treated with 5 % sodium hypochlorite solution (Commercial Bleach) for 4 hours to expose the epiphyseal and metaphyseal trabecular bone. Specimens were placed into 2.5 % buffered glutaraldehyde solution. Tissues were dehydrated by using acetone series with increasing degree. After the drying process, they were mounted on aluminum reservoirs by liquid silver and coated with gold/palladium in Denton Vacuum, LLC Desk V sputter/etch unit coating device (Denton vacuum LLC, Moorestown, NJ) (Panwar *et al.*, 2013). The tissue loaded was evaluated and captured using a scanning electron microscope (JEOL, JSM-5200).

**Statistical Analysis.** Statistical analysis was carried out using SPSS v. 15 software. All data were expressed as means  $\pm$  standard error of mean (SEM). The data were analyzed by one-way analysis of variance (ANOVA) followed by Duncan test to determine difference between groups. P values of less than 0.05 were considered statistically significant.

## RESULTS

Histological sections of the middle shaft of femur from rats of the sham-operated control group showed that bone tissue was of the compact type, covered by two layers, the periosteum found remotely, which is a thick connective tissue, and the endosteum, a flimsy cell-rich connective tissue, coating the inside surface of the bone confronting the bone marrow cavity. At the outer edges of compact bone, rather than being settled in osteons, the osseous tissue is organized in circumferential lamellae. Within the bone matrix, osteocytes are originated in lacunae, which are the cell-shaped empty spaces that prevent the solid, mineralized extracellular material of bone from pounding the osteocytes. At the middle of each osteon is a Haversian canal through which blood vessels, lymph vessels, and nerves can travel to facilitate and signal the cells throughout the compact bone were detected (Fig. 1A). The head of the femur bone was made of cancellous bone. Trabeculae of the cancellous bone of sham control rats were composed of a network of irregular bone lamellae between which osteocytes resided in their lacunae. It revealed normal architecture of dense and uniform trabeculae (TB). Moreover, intertrabecular spaces and bone marrow (BM), were observed to be normal (Fig. 1B). The osteoblastic cover oscillated from cuboidal cells with large nuclei to thin cells with fusiform nuclei and responsible for synthesizing the organic components of the bone was observed (Figs. 1B and 1C). Osteoblasts also give rise to osteocytes which surrounded by newly deposited organic matrix (Fig. 1D).

In the case of OCX rats, examination of the middle shaft of the femur showed marked decrease in the thickness of the compact bone of the shaft of the sham-operated group and decrease in the number of osteocytes. Examined sections of model group showed osteodystrophy fibrosa, resulting in a loss of bone mass, a weakening of the bones as their calcified supporting structures are replaced with fibrous tissue (Fig. 2A). Many osteoporotic cavities, resorption cavities were observed in bone tissue (Fig. 2A). The middle shaft of the femur showed fragmented bone matrix and activation of a large multinucleated osteoclasts which are responsible for the dissolution and absorption of bone (Fig. 2B). Mineralized bone is first broken into fragments; the osteoclast then engulfs the fragments and digests them within cytoplasmic vacuoles.

Histological section of OCX rats cancellous bone in the head of the femur revealed marked disruptive changes of bone structure including widening of intertrabecular spaces at the expense of the trabecular width when compared to sham control rats. Some trabeculae suffered from necrosis of osteocytes and osteoblasts showing karyopyknosis and karyolysis (Fig. 2C). Induced osteoporosis by orchietomy

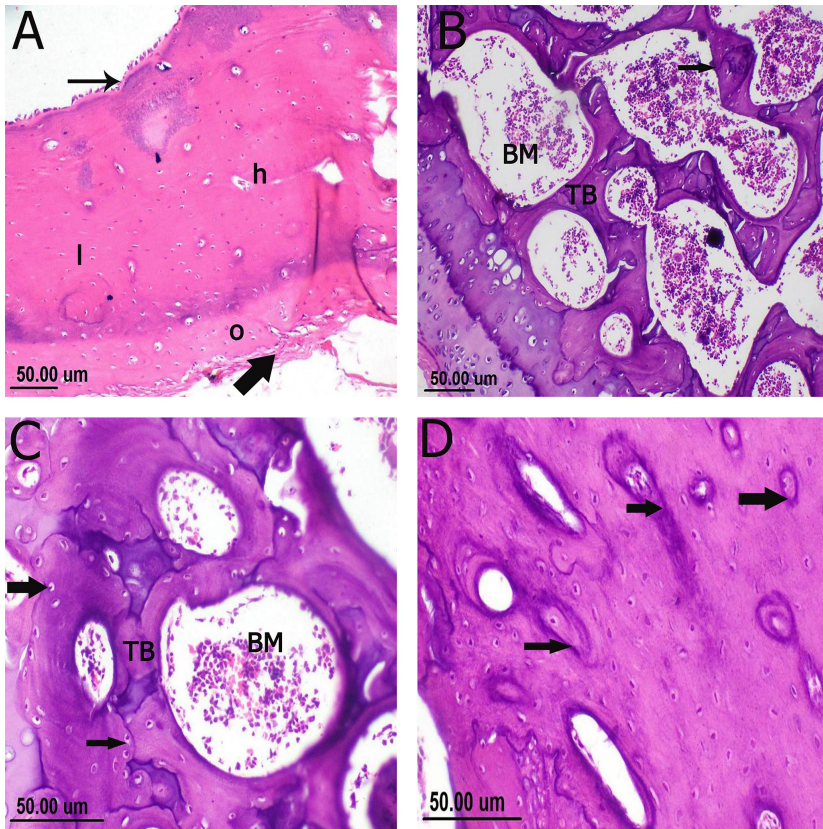


Fig. 1. Photomicrographs of the rat femur stained by hematoxylin and eosin showing compact and cancellous bone structure of Sham (control) group: (A) Represents a normal bone tissue of the compact type, covered by two layers, the periosteum (thick arrow) located externally and the endosteum (thin arrow). At the outer edges of compact bone, the osseous tissue is arranged in outer circumferential lamellae (O). Osteocytes are found in lacunae (l). At the center of each osteon is a Haversian canal (h). (B) Revealed normal architecture of trabecular bone (TB) surround bone marrow (BM). The arrow refers to osteoblastic cover. (C) Shows the bone forming osteoblasts (arrows) located on the surface of the trabeculae (TB) which surround bone marrow (BM). (D) Shows osteocytes which surrounded by newly deposited organic matrix (arrows). (Bar = 50  $\mu$ m).

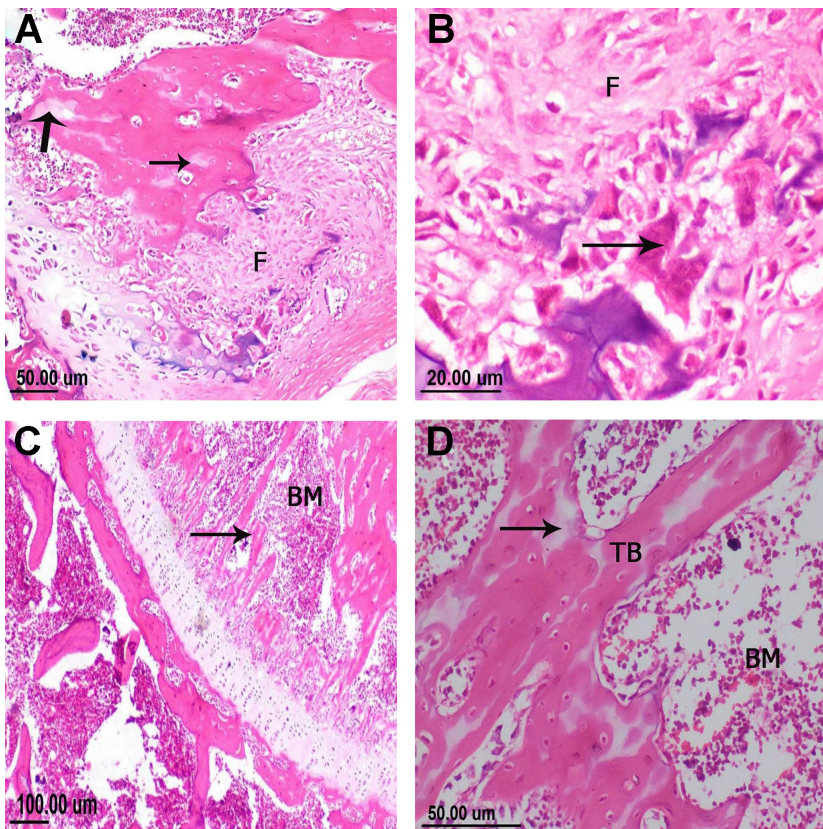


Fig. 2. Photomicrographs of the rat femur stained by hematoxylin and eosin showing compact and cancellous bone structure of OCX group: (A) Shows osteodystrophy fibrosa (F), many osteoporotic cavities in bone tissue (arrows). (Bar = 50  $\mu$ m). (B) Shows fragmented bone matrix and osteoclastic activity (arrow), responsible for osteodystrophy fibrosa (F). (Bar = 20  $\mu$ m). (C) Some trabeculae suffered from necrosis (arrow). Moreover, a marked reduction in the trabecular area, and increase in blood vascularity within the bone marrow (BM). (Bar = 100  $\mu$ m). (D) Shows increase of osteoporotic cavities (arrow), and the trabeculae (TB) were thin with decrease bone density surrounded bone marrow (BM). (Bar = 50  $\mu$ m).

leads to an increase of osteoporotic cavities, erosion cavities were detected on the outer surface and the trabeculae were thin with decrease bone density (Fig. 2D).

Examination of bone sections of the middle shaft in OCX rats treated with *Allolobophora caliginosa* extract (AcE) (100 mg/kg body weight/day) (T1 group) showed increase in the thickness of the shaft cortical bone and significant restorative changes with normal size and shape of active osteoblasts compared to the OCX group. The number of osteocytes was also increased, as compared with OCX rats. But, many osteoporotic cavities, resorption cavities were observed in bone tissue (Fig. 3A).

In the head of the femur of this group, decreased areas of bone trabeculae were observed compared to the sham-operated group. However, slight increase in areas of bone trabeculae was seen compared to OCX rats. Bone sections showed active growth plate (Fig. 3B).

In case of OCX rats treated with (AcE) (200 mg/kg body weight/day) (T2 group), an improvement was seen in pathological changes in the form of increase in cortical bone thickness of the middle shaft as compared to the OCX group, and the number of osteocytes returned to normal. Bone tissue was covered by the periosteum and below it the bone forming osteoblasts appeared cuboidal with large nuclei (Fig. 3C). Osteocytes are found in lacunae, and at the center of each osteon is a Haversian canal were detected (Fig. 3C).

Significant increase in areas of bone trabeculae of this group showed preserved architecture, seems to have the better connected trabecular bone structure, leads to a decrease of intertrabecular cavities, were seen compared to OCX rats (Fig. 3D).

The growth plate in this group showed different healthy zones of cartilage, revealed an improvement in histological changes (Fig. 3D).

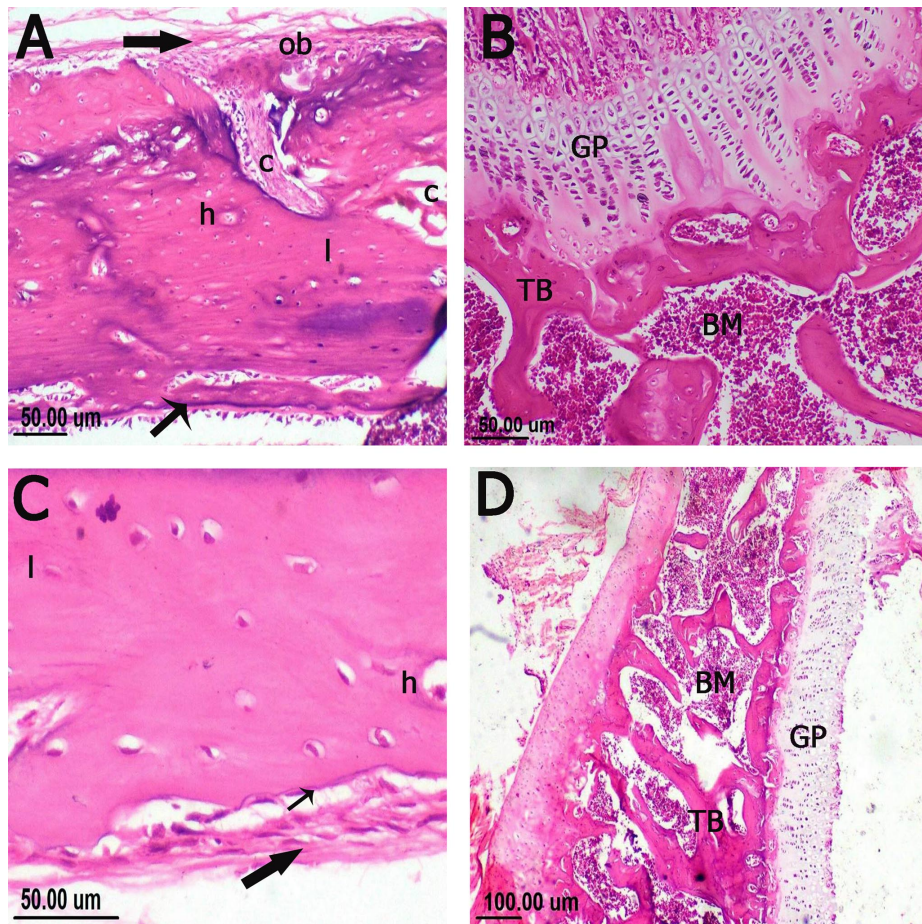


Fig. 3. Photomicrographs of the rat femur stained by hematoxylin and eosin showing compact and cancellous bone structure of OCX rats treated with ACE (100 mg/kg body weight/day) group (A) and (B) and OCX rats treated with ACE (200 mg/kg body weight/day) group (C) and (D): (A) Represents that bone tissue was of the compact type, covered by two layers, the periosteum (thick arrow) and the endosteum (thin arrow), significant restorative changes with normal size and shape of active osteoblasts (ob). Osteocytes inside lacunae (l) surround Haversian canal (h). Many osteoporotic cavities were still present (c). (Bar = 50 μm). (B) Shows slight increase in areas of bone trabeculae (TB), which surround bone marrow (BM) and active growth plate (GP). (Bar = 50 μm). (C) Shows that the compact bone covered by two layers, the periosteum located externally (arrow), and below it the bone forming osteoblasts (thin arrow). Osteocytes are found in lacunae (l), at the center of each osteon is a Haversian canal (H). (Bar = 50 μm). (D) Shows preserved architecture of trabeculae (TB), surround bone marrow (BM). The

**Scanning Electron Microscopic (SEM) examination.** The connectivity of femoral trabecular bone exhibited greater connection without resorption cavities in sham-operated control group (Figs. 4A and 4B). Conversely, orchietomy caused alterations of normal bone architecture such as a decrease in femoral trabecular bone and disintegration in bone architecture, combined with resorption cavities and various holes, thinning, tapering, breakage, and perforation made the arch structure lose its integrity as compared to sham control rats (Figs. 4C and 4D). Administration of (AcE) in

T1 group rats alleviated the abnormalities induced by orchietomy; on the bottom of the lacuna, tight or loose collagen fibrils presented and improved bone architecture near to normal pattern, as compared to OCX rats (Figs. 4E and F). Furthermore, administration of (AcE) in T2 group rats ameliorated the changes of trabecular bone caused by orchietomy and its morphology remained nearly normal, improved the collagen, as indicated by the reduction in holes and the arrangement of fibrillar collagen in comparison with untreated OCX rats (Figs. 4G and H).

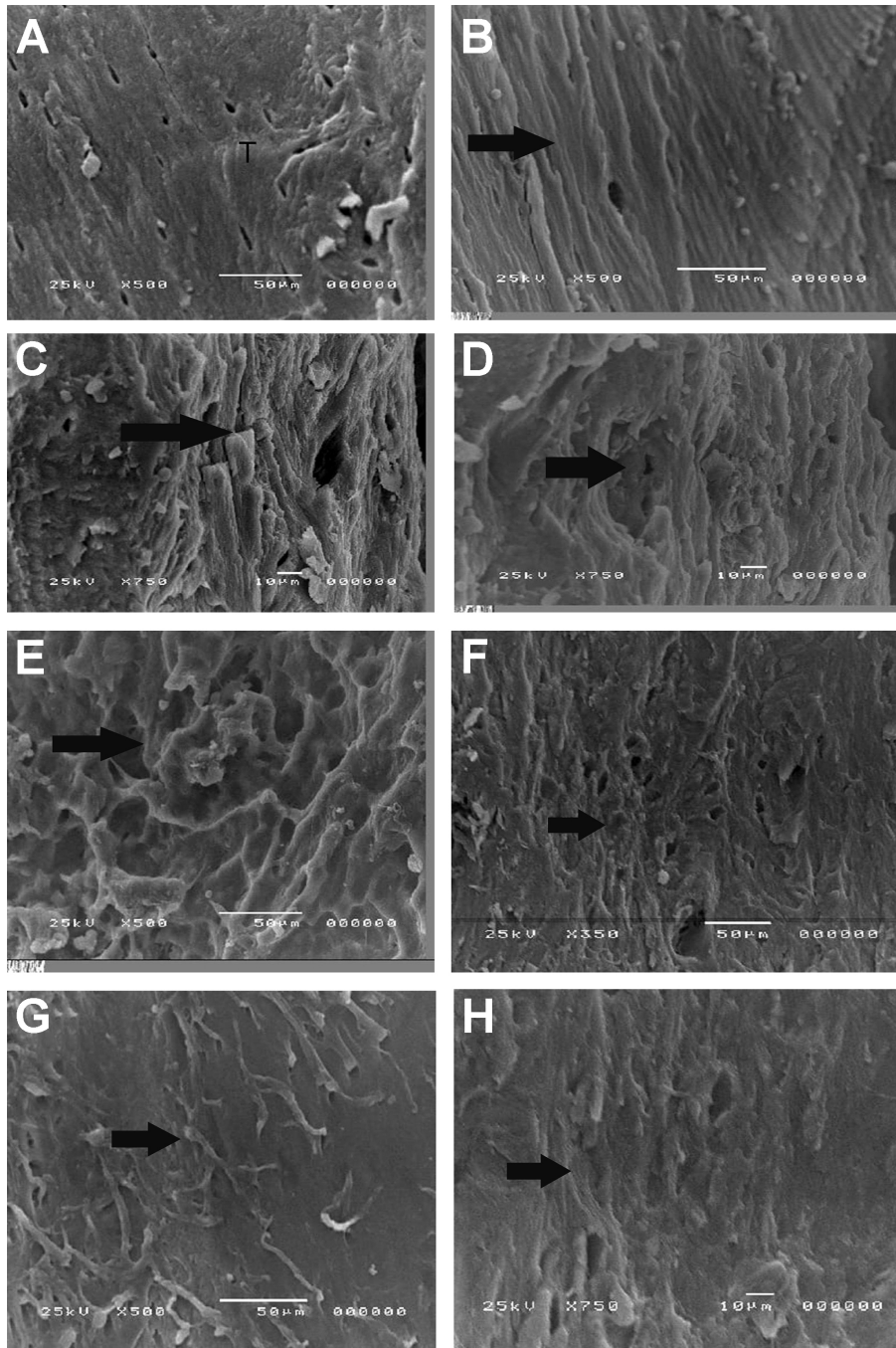


Fig. 4. Scanning electron micrographs of the femoral proximal metaphysis in rats. A) Sham group, represents the normal bone structure and trabecular integrity (T). (bar = 50 µm). B) The connectivity of trabecular bone in the metaphysis exhibited greater connection in the sham control group (arrow). (bar = 50 µm). C) OCX group showing a decrease in femoral trabecular bone and disintegration in bone architecture (arrow) (bar = 10 µm). D) OCX group showing trabecular disconnection and degeneration (arrow). (bar = 10 µm). E) T1 group showing more or less regeneration of trabecular structure, as compared with the OCX group (bar = 50 µm). F) T1 group alleviated the abnormalities induced by orchietomy; and improved bone architecture near to normal pattern (arrow). (bar = 50 µm). G) T2 group showing cancellous bone pattern similar to the normal bone pattern. and numerous normal connections were observed (arrow). (bar = 50 µm). H) T2 group showing the normal structure of femoral metaphysis (arrow). (bar = 10 µm).

**Immunohistochemical analysis:** Immunohistochemical examination for caspase-3 and Bcl2 proteins was conducted in femoral bone tissue of the different studied groups. The expression of caspase-3 was weakly detected in sham-operated control group. In contrast, OCX group showed heavy expression in the osteoblasts. Moderate number of positive cells was observed in T1 and T2 groups (Figs. 5 and 6). Concerning Bcl2 immune staining, strong expression

was detected in sham-operated control group. Meanwhile, OCX group revealed weak staining. Increased expression of Bcl2 was noticed in T1 and T2 groups compared to model group. The statistical analysis of area % expression of caspase-3 showed a significant decrease in treated group compared to OCX group. However, expression of Bcl2 exhibited a significant increase in treated groups compared to OCX group (Figs. 5 and 7).

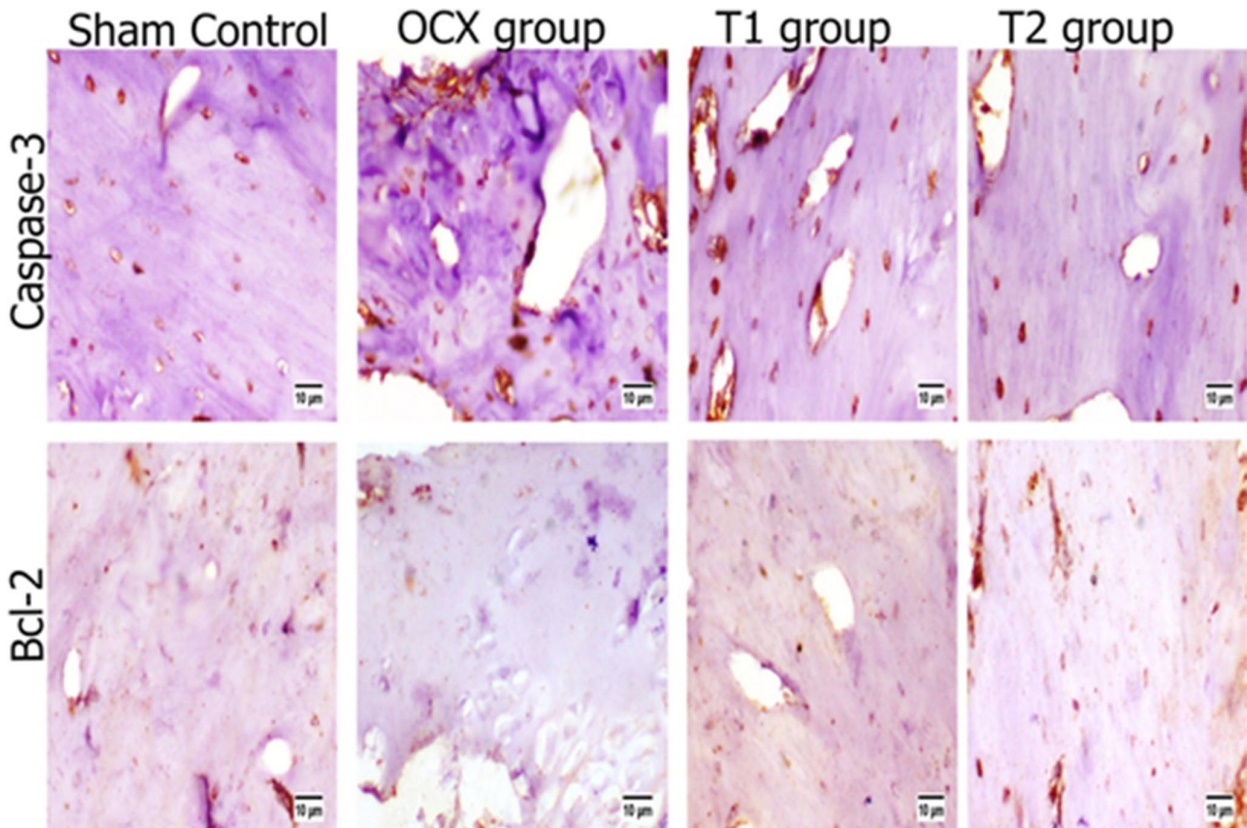


Fig. 5. Immunohistochemical staining of caspase-3 and Bcl2 in studied groups.

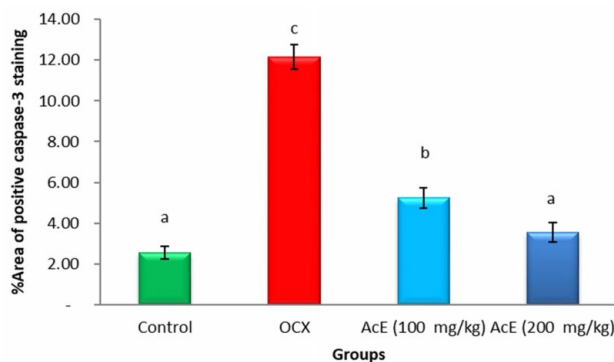


Fig. 6. Charts showing area % expression of caspase-3 in different groups. Data Expressed as means  $\pm$  standard error. Significant difference was considered at  $p < 0.05$ .

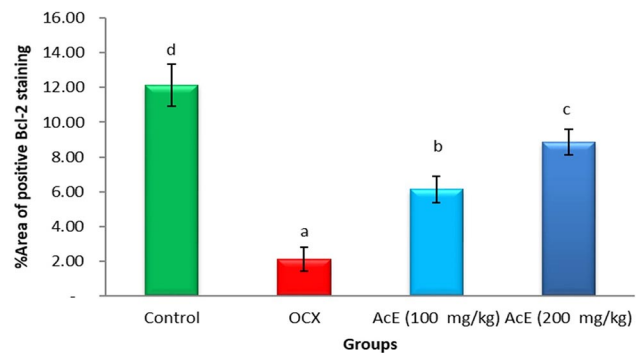


Fig. 7. Charts showing area % expression of Bcl-2 in different groups. Data Expressed as means  $\pm$  standard error. Significant difference was considered at  $p < 0.05$ .

## DISCUSSION

Osteoblasts are bone cells that synthesize the organic matrix and control the mineralization process while Osteoclasts causes bone resorption (Bai *et al.*). Osteoporosis is caused by a decrease in the number of osteoblasts, which results in a decrease in bone mineralization and creation. Lock *et al.* (2006) said that osteoporosis is a multifactorial disease that is linked to demographic and lifestyle factors, as well as morbidity, substance use, medical history, and hormonal changes.

In the present study, orchietomy of rats induced a decrease in thickness of the shaft cortical bone and in the number of osteocytes, also revealed noticeable resorption and reduction in the thickness of bony trabeculae causing widening of the bone marrow spaces compared to sham operated controls. The study of Shata *et al.* (2015) also showed similar results, where they found that the femoral cancellous bone showed severe bone resorption in the form of marked thinning and irregularity of the bone trabeculae. There were studies regarding histological comparisons of normal versus osteoporotic bones (Suvorova *et al.*, 2007; Qaseem *et al.*), they found that there was cortical effacement and reduction in the density and integrity of trabecular bone in patients with osteoporosis. Many osteoporotic cavities were also seen in the group of OCX rats compared to sham operated controls. Oktem *et al.* (2006) have explained that the pathogenesis of OP produces a free radical, which contributes to the estrogen-induced imbalance in bone formation and resorption.

Early differentiation of osteoblasts was stimulated by earthworm extract, which is beneficial for osteoblast mineralization (Fu *et al.*). Earthworm extract inhibits osteoclastogenesis transcription by inhibiting cFos expression (Dharmawati *et al.*, 2020). In the present study, bone sections of OCX rats treated with AcE at Dose 200 mg/kg/day level was found effective and highly significant showed marked increase in the thickness of the cortical bone, that prevented cortical as well as trabecular bone loss where Dose (100 mg/kg/day) was observed moderately significant, slight increase in the thickness of the cortical bone, that prevented cortical as well as trabecular bone loss compared to that in OCX rats, may be due to enhancement of osteoblastic activity and reduction of osteoclastic activity. This may indicate significant effect of AcE on osteoporotic bone. Our results were in accordance with the previous studies which reveal that the capacity to form matrix mineralization was positively correlated with osteoblast proliferation and differentiation (Fu *et al.*). Moreover, Grdisa *et al.* (2004) found that glycolipid protein extract from the

earthworm had a protective effect against H<sub>2</sub>O<sub>2</sub> toxicity and stimulated the growth of human fibroblasts and epithelial cells. Recent investigations have discovered that lumbrokinase protects against hippocampus apoptosis, have therapeutic potential in diabetic nephropathy, and have anti-ischemic properties in the brain (Huang *et al.*, 2013).

In the present study, at the SEM level all trabecular structure in the OCX group was degenerated and thinned. This finding suggested that changes in internal structure of trabecula might be caused by degenerated collagen structure. On SEM evaluation, it was reported that trabeculae of T1 group alleviated the abnormalities induced by orchietomy; on the bottom of the lacuna and improved bone architecture. Furthermore, the T2 group strengthened the collagen, as shown by the reduction in holes and the arrangement of fibrillar collagen, and the changes in trabecular bone induced by orchietomy were mitigated and its morphology remained nearly usual in comparison to untreated OCX rats. Our investigations are in accordance with the previous studies of Shen *et al.* (2009), Suvorova *et al.* and Raguin *et al.* (2021).

Caspase-3 and Bcl-2 are pro-apoptotic and anti-apoptotic regulatory proteins, respectively that work as pairs to regulate the apoptosis occurrence and progression (Kale *et al.*; Badr *et al.*). Bcl-2 prevents apoptotic cell death by inhibiting the release of apoptogenic factors including cytochrome c and apoptosis-inducing factor from the mitochondrial intermembrane space (Tsujiyama & Shimizu, 2000). Furthermore, the activation of caspase-3, an apoptotic marker, means that the cell has died irreversibly (Badr *et al.*). It is well established that oxidative stress is frequently responsible for the mitochondria-mediated apoptosis signalling pathway and that high levels of ROS reduce Bcl-2 expression, resulting in increased cytochrome c release, which promotes caspase-3 activation and apoptotic cell death (Rana, 2008). The present study showed an increased number of apoptotic osteoblasts in the OCX rats, perhaps via the imbalance between pro- and anti-apoptotic proteins, in accordance with the previous studies of Kogianni *et al.* (2004) who demonstrated that cell apoptosis occurred in steroid-induced femoral head necrosis from the perspective of Fas cell surface death receptor/CD95 and Kabata *et al.* (2000) who demonstrated that a large number of osteoblasts and osteoclasts become apoptotic, and, as apoptosis continues, osteoporosis is caused.

The present study indicated that the number of apoptotic cells was decreased in *Allolobophora caliginosa* extract (AcE) T1 and T2 groups and reduced the expression of Caspase-3 and increased the expression of Bcl-2, an inhibitor of cell apoptosis. These results in accordance with the previous studies of Hay *et al.* (2001) and Dharmawati *et al.*

From the results of this study can prove that AcE provides good anti-osteoporotic and antiapoptotic activity against orchietomized rat model. Therefore, AcE may be used for the prevention of steroid-induced bone damage.

**MAGDY, A.; FAHMY, S. R.; MOHAMED, A. S.; SAAD, D. Y.; DESOKYAND, R. S. & BAIOMY, A. A. A.** Estudio histopatológico e inmunohistoquímico de la eficacia antiosteoporótica del extracto de lombriz de tierra *Allolobophora caliginosa* en ratas orquiectomizadas. *Int. J. Morphol.*, 40(1):277-286, 2022.

**RESUMEN:** La osteoporosis es una afección ósea caracterizada por una pérdida de masa ósea y una alteración de la microarquitectura ósea. Los hombres pierden densidad ósea a medida que envejecen, lo que resulta en huesos quebradizos. La pérdida de testosterona libre es factor clave en este proceso. El objetivo del presente estudio fue evaluar el extracto de *Allolobophora caliginosa* (AcE) debido a su actividad antiosteoporótica y antiapoptótica en un modelo de rata orquiectomizadas con dos niveles de dosis diferentes. Se dividieron veintiocho ratas macho en dos grupos. El primer grupo incluyó ratas con operación simulada, mientras que el segundo grupo se sometió a orquidectomía bilateral (OCX). Después de una semana de recuperación de la orquidectomía, el segundo grupo fue subdividido en 3 subgrupos. Al primer subgrupo de OCX se administró diariamente agua destilada por vía oral durante 10 semanas. Los otros dos subgrupos de OCX se administraron por vía oral AcE (100 o 200 mg / kg de peso corporal / día) durante 10 semanas. La orquidectomía induce una pérdida notable del hueso cortical y trabecular; el cual podría ser contrarrestado por el extracto de *Allolobophora caliginosa* (AcE) que previno la pérdida de hueso tanto cortical como trabecular visualizado en imágenes histológicas y estudio inmunohistoquímico, donde se encontró que la dosis (100 mg / kg / día) era moderadamente significativa. En el presente estudio, se sugiere que la AcE puede inhibir la apoptosis de los osteoblastos inducida por esteroides, potencialmente a través de la regulación al alza de Bcl 2 y la regulación a la baja de caspasa 3. El extracto de *Allolobophora caliginosa* demuestra propiedades anti apoptóticas y antioxidantes. Por lo tanto, AcE puede usarse para la prevención del daño óseo inducido por esteroides.

**PALABRAS CLAVE:** Osteoporosis; Extracto de *Allolobophora caliginosa*; Rata orquiectomizada; Histopatología; Apoptosis

## REFERENCES

Badr, A. M.; Farid, M.; Biomy, A. A. A.; Mohamed, A. S.; Mahana, N. A. & Fahmy, S. R. Protective effect of *Toxocara vitulorum* extract against alphanaphthylisothiocyanate-induced cholangitis in rat. *J. Basic Appl. Zool.*, 81:62, 2020

Bai, J.; Xu, Y.; Diao, Y. & Sun, G. Combined low-dose LiCl and LY294002 for the treatment of osteoporosis in ovariectomized rats. *J. Orthop. Surg. Res.*, 14(1):177, 2019.

Baiomy, A. A. & Mansour, A. A. Genetic and histopathological responses to cadmium toxicity in rabbit's kidney and liver: protection by ginger (*Zingiber officinale*). *Biol. Trace Elem. Res.*, 170(2):320-9, 2016.

Bin Dajem, S.; Ali, S.; Abdelrady, O.; Salahaldin, N.; Soliman, A.; Kamal, Y.; Abdelazim, A. Y.; Mohamed, A. F.; Morsy, K.; Mohamed, A. S.; *et al.* *Allolobophora caliginosa* coelomic fluid ameliorates gentamicin-induced hepatorenal toxicity in rats. *Asian Pac. J. Trop. Biomed.*, 10(9):411-6, 2020.

Chen, J. S. & Sambrook, P. N. Antiresorptive therapies for osteoporosis: a clinical overview. *Nat. Rev. Endocrinol.*, 8(2):81-91, 2011.

Dharmawati, I. A.; Sukrama, I. D. M.; Bakta, I. M.; Manuaba, I. B. P.; Thahir, H.; Astawa, I. N. M. & Kartini, N. L. Effectiveness of *Lumbricus rubellus* earthworm extract against the number of osteoclasts in Wistar periodontitis rat. *Eur. J. Mol. Clin. Med.*, 7(11):1584-92, 2020.

Duque, G. & Troen, B. R. Understanding the mechanisms of senile osteoporosis: new facts for a major geriatric syndrome. *J. Am. Geriatr. Soc.*, 56(5):935-41, 2008.

Fu, Y. T.; Chen, K. Y.; Chen, Y. S. & Yao, C. H. Earthworm (*Pheretima aspergillum*) extract stimulates osteoblast activity and inhibits osteoclast differentiation. *BMC Complement. Altern. Med.*, 14:440, 2014.

Fui, M. N. T.; Hoermann, R.; Nolan, B.; Clarke, M.; Zajac, J. D. & Grossmann, M. Effect of testosterone treatment on bone remodelling markers and mineral density in obese dieting men in a randomized clinical trial. *Sci. Rep.*, 8:9099, 2018.

Grdisa, M.; Popovic, M. & Hrzenjak, T. Stimulation of growth factor synthesis in skin wounds using tissue extract (G-90) from the earthworm *Eisenia foetida*. *Cell Biochem. Funct.*, 22(6):373-8, 2004.

Hassanein, E. H. M.; Shalkami, A. G. S.; Khalaf, M. M.; Mohamed, W. R. & Hemeida, R. A. M. The impact of Keap1/Nrf2, P38 MAPK/NF- $\kappa$ B and Bax/Bcl2/caspase-3 signaling pathways in the protective effects of berberine against methotrexate-induced nephrotoxicity. *Biomed. Pharmacother.*, 109:47-56, 2019.

Hay, E.; Lemonnier, J.; Fromigué, O. & Marie, P. J. Bone morphogenetic protein-2 promotes osteoblast apoptosis through a Smad-independent, protein kinase C-dependent signaling pathway. *J. Biol. Chem.*, 276(31):29028-36, 2001.

Hrzenjak, T.; Hrzenjak, M.; Kasuba, V.; Efenberger-Marinculic, P. & Levanat, S. A new source of biologically active compounds--earthworm tissue (*Eisenia foetida*, *Lumbricus rubellus*). *Comp. Biochem. Physiol. Comp. Physiol.*, 102(3):441-7, 1992.

Huang, C. Y.; Kuo, W. W.; Liao, H. E.; Lin, Y. M.; Kuo, C. H.; Tsai, F. J.; Tsai, C. H.; Chen, J. L. & Lin, J. Y. Lumbricin attenuates side-stream-smoke-induced apoptosis and autophagy in young hamster hippocampus: correlated with eNOS induction and NF $\kappa$ B/iNOS/COX-2 signaling suppression. *Chem. Res. Toxicol.*, 26(5):654-61, 2013.

Kabata, T.; Kubo, T.; Matsumoto, T.; Nishino, M.; Tomita, K.; Katsuda, S.; Horii, T.; Uto, N. & Kitajima, I. Apoptotic cell death in steroid induced osteonecrosis: an experimental study in rabbits. *J. Rheumatol.*, 27(9):2166-71, 2000.

Kale, J.; Osterlund, E. J. & Andrews, D. W. BCL-2 family proteins: changing partners in the dance towards death. *Cell Death Differ.*, 25(1):65-80, 2018.

Khosla, S. Update in male osteoporosis. *J. Clin. Endocrinol. Metab.*, 95(1):3-10, 2010.

Kogianni, G.; Mann, V.; Ebetino, F.; Nuttall, M.; Nijweide, P.; Simpson, H. & Noble, B. Fas/CD95 is associated with glucocorticoid-induced osteocyte apoptosis. *Life Sci.*, 75(24):2879-95, 2004.

Kuehn, B. M. Long-term risks of bisphosphonates probed. *JAMA*, 301(7):710-1, 2009.

Kumar, G. S. *Preparation of Specimens for Histologic Study*. In: Kumar, G. S. & Bhaskar, S. N. (Ed.). *Orban's Oral Histology & Embryology*. 13th ed. New Delhi, Elsevier Health Sciences, 2014. pp.410-6.

Li, M. & Zhong, M. Bisphosphonates and risk of oesophageal cancer: A meta-analysis. *GastroHep*, 2(3):123-32, 2020.

Lock, C. A.; Lecouturier, J.; Mason, J. M. & Dickinson, H. O. Lifestyle interventions to prevent osteoporotic fractures: a systematic review. *Osteoporos. Int.*, 17(1):20-8, 2006.

- Oktem, G.; Uslu, S.; Vatanserver, S. H.; Aktug, H.; Yurtseven, M. E. & Uysal, A. Evaluation of the relationship between inducible nitric oxide synthase (iNOS) activity and effects of melatonin in experimental osteoporosis in the rat. *Surg. Radiol. Anat.*, 28(2):157-62, 2006.
- Panwar, P.; Du, X.; Sharma, V.; Lamour, G.; Castro, M.; Li, H. & Brömme, D. Effects of cysteine proteases on the structural and mechanical properties of collagen fibers. *J. Biol. Chem.*, 288(8):5940-50, 2013.
- Qaseem, A.; Forciea, M. A.; McLean, R. M.; Denberg, T. D.; Clinical Guidelines Committee of the American College of Physicians; Barry, M. J.; Cooke, M.; Fitterman, N.; Harris, R. P.; Humphrey, L. L.; *et al.* treatment of low bone density or osteoporosis to prevent fractures in men and women: a clinical practice guideline update from the American College of Physicians. *Ann. Intern. Med.*, 166(11):818-39, 2017.
- Rana, S. V. S. Metals and apoptosis: recent developments. *J. Trace Elem. Med. Biol.*, 22(4):262-84, 2008.
- Saki, F.; Kasaei, S. R.; Sadeghian, F.; Talezadeh, P. & Omrani, G. H. R. The effect of testosterone itself and in combination with letrozole on bone mineral density in male rats. *J. Bone Miner. Metab.*, 37(4):668-75, 2019.
- Sakr, H. F.; Hussein, A. M.; Eid, E. A.; Boudaka, A. & Lashin, L. S. Impact of Dehydroepiandrosterone (DHEA) on bone mineral density and bone mineral content in a rat model of male hypogonadism. *Vet. Sci.*, 7(4):185, 2020.
- Shata, A.; Firgany, A. E. L. & Abdel-Hamid, A. A. M. Ameliorating effect of combination of simvastatin and Risedronate on glucocorticoid induced osteoporosis model in rats. *Afr. J. Pharm. Pharmacol.*, 9(28):701-10, 2015.
- Suvorova, E. I.; Petrenko, P. P. & Buffat, P. A. Scanning and transmission electron microscopy for evaluation of order/disorder in bone structure. *Scanning*, 29(4):162-70, 2007.
- Tsujimoto, Y. & Shimizu, S. Bcl-2 family: life-or-death switch. *FEBS Lett.*, 466(1):6-10, 2000.

Corresponding author:  
Ahmed Abdel Aziz Baiomy  
Zoology Department  
Faculty of Science  
Cairo University  
Giza 12316  
EGYPT

Email: aabdelaziz.baiomy@gmail.com  
aabdelaziz.baiomy@cu.edu.eg